The Astrophysical Journal, 593:630–639, 2003 August 20


# LUMINOUS LYMAN BREAK GALAXIES AT $z > 5$ AND THE SOURCE OF REIONIZATION[1]

Matthew D. Lehnert[2] and Malcolm Bremer[3]

*Received 2003 February 4; accepted 2003 April 23*


## ABSTRACT

We have discovered six galaxies with spectroscopically confirmed redshifts of $4.8 < z < 5.8$ in a single 44 arcmin$^2$ field deeply imaged in $R$, $I$, and $z$ bands. All the spectra show an emission line in the region around 7000–8400 Å with a spectroscopically detected faint continuum break across the line. These six were drawn from 13 sources with $I_{AB} < 26.2$ and $R_{AB} - I_{AB} > 1.5$ in the field; this photometric cut is designed to select galaxies at $z > 4.8$. The line fluxes range between 0.2 and $2.5 \times 10^{-17}$ ergs cm$^{-2}$ s$^{-1}$, indicating luminosities of around $10^{42}$–$10^{43}$ ergs s$^{-1}$ for Ly$\alpha$, and their high emission line equivalent widths suggest very young ages ($\lesssim 10^8$ yr). A further line-emitting object with no detectable continuum was serendipitously detected by spectroscopy. If this line is Ly$\alpha$, then it is from a source at $z = 6.6$, making this the most distant galaxy known. However, the redshift cannot be considered secure as it is based on a single line. No broad emission line objects (quasars) were detected. The 13 sources at $I_{AB} < 26.2$ are less than that expected if the luminosity function of dropout galaxies remained unchanged between $z = 3$ and 6, although the deficit is not highly significant given possible cosmic variance. The UV luminosity density from galaxies brighter than our flux limit is considerably less than that necessary to keep the volume probed by our field at $\langle z \rangle \sim 5.3$ ionized. These galaxies are observed within several hundred megayears of the end of the epoch of reionization ($z = 6$–7), with little time for the luminosity function to evolve. This and the lack of detected quasars imply that the bulk of the UV flux that reionized the universe came from faint galaxies with $M_{AB}(1700\ \text{Å}) > -21$.


*Subject headings:* cosmology: observations — early universe — galaxies: distances and redshifts — galaxies: evolution — galaxies: formation

*On-line material:* color figures

## 1. INTRODUCTION

While progress has been made in our understanding of how galaxies formed and evolved by studying the dynamics, morphologies, and stellar populations of low-redshift galaxies, a complete physical picture can be obtained only by actually witnessing the important physical processes in situ. With this in mind there has been an explosion in the number of galaxies and quasi-stellar objects (QSOs) discovered at the highest redshifts ($z > 5$: e.g., Hu et al. 2002; Ellis et al. 2001; Stern & Spinrad 1999; Dey et al. 1998; Fan et al. 2001; Rhoads et al. 2003). These galaxies have been found using a variety of techniques ranging from narrowband imaging, to accidental alignments of spectroscopic slits on high-redshift objects, to using the dropout technique (Lyman break galaxies; LBGs) pioneered by Steidel et al. (1999). Such a diverse approach is necessary in order to make a full census of the high-redshift population. Without such a census, it is impossible to elucidate the physical processes that drive galaxy evolution at the highest redshifts. Moreover, to find the objects that may have reionized the universe probably means that we will have to obtain a full luminosity function of the most plausible objects such as QSOs, massive stars in galactic fragments, or perhaps even something more exotic (e.g., Loeb & Barkana 2001).

In the present paper, we describe a program to find faint continuum-emitting objects at $z \approx 5.5$. Our hope was to detect objects at an epoch close enough to that of reionization so that we could determine whether UV-luminous galaxies or quasars caused the reionization. We selected a redshift range that is lower than what is generally considered appropriate for the complete reionization of the universe (see review by Loeb & Barkana 2001; Fan et al. 2001), because before the universe is substantially ionized, Ly$\alpha$ may be effectively suppressed by resonant scattering of the Ly$\alpha$ by the neutral intergalactic medium or by the damping wings of a largely neutral medium. Thus at or before the epoch of reionization, there may be no observable Ly$\alpha$ emission with which to obtain redshifts. Also, the ionizing photon density necessary to reionize the intergalactic medium increases as $(1 + z)^3$ (Madau, Haardt, & Rees 1999), and it is unlikely that the ionizing photon output of the LBGs was the source of reionization even if such output remained constant from $z = 3$ to the reionization at $z > 6$ (Ferguson, Dickinson, & Papovich 2002). Moreover, the timescale between redshifts of 5.5 and 7–10, which is the current best estimate for when reionization likely occurred (Loeb & Barkana 2001 and references therein), is less than several hundred megayears for any reasonable cosmology. Over such a short timescale, while individual galaxies may evolve rather dramatically, it is unlikely that the galaxy number density could evolve very strongly (hierarchical merger models suggest that it is likely only to be a factor of a few: e.g., Sokasian et al. 2003; Ciardi, Stoehr, & White 2003). Given these competing constraints, gauging the ionizing photon density at high redshifts soon after the likely epoch of reionization may provide a highly significant determination of the types of galaxies that were responsible for reionization. Therefore, for the source of ionization to be galaxies, we seek a population of galaxies that are still line

[1] Based on observations collected at the Very Large Telescope branch of the European Southern Observatory, Cerro Paranal, Chile.

[2] Max-Planck-Institut für extraterrestrische Physik, Giessenbachstrasse, 85748 Garching bei München, Germany.

[3] Department of Physics, Bristol University, H. H. Wills Physics Laboratory, Tyndall Avenue, Bristol BS8 1TL, UK.

emitting (i.e., actively forming stars), with a UV photon density sufficient to keep the intergalactic medium (IGM) ionized at the observed epoch and with significant UV continua suggestive of prolonged star formation (Leitherer et al. 1999; Sullivan et al. 2000), which is sufficient to ionize the IGM at higher redshifts. If reionization is due to QSOs, then we would need to observe many more QSOs than would be predicted by extrapolating to low luminosity the QSO luminosity function of Fan et al. (2001) for very luminous QSOs ($M_B \lesssim -26$).

## 2. OBSERVATIONS AND OBJECT SELECTION

### 2.1. *Broadband Observations*

We obtained deep multicolor broadband observations of an approximately 44 arcmin$^2$ field using the imaging spectrograph FORS2 on UT4 of the Very Large Telescope (VLT). The field was chosen to have minimal extinction from the maps of Schlegel, Finkbeiner, & Davis (1998), had low (cirrus) 100 $\mu$m emission, was south of the latitude of the VLT (to point out of the prevailing winter wind), and was easily observable from June to October. The data were obtained in "service mode" on the nights of 2002 June 17, July 6, 7, and 12. The data were taken as a sequence of dithered exposures with a net integration time of 2.6 hr in $R$ and 1 hr each in the $I$ and $z$ bands. The images were processed in the standard way but were flat-fielded using images generated by masking out all pixels with surface brightnesses between $\pm 3$ $\sigma$ of the background noise and then averaged without the images being aligned. Constructing the flat-field frame in this manner resulted in final images that are characterized by background levels across the image that are flat to within much better than 1% of the average value. The final combined image had a noise level consistent with that expected from Poissonian statistics given the sky background and number of individual exposures. Conditions were photometric throughout the observations. The final calibration was determined through observations of stars in the field of PG 1323−086 and Mrk A (Landolt 1992) for the $R$ and $I$ filters and by observations of the spectrophotometric standard LTT 377 (Hamuy et al. 1994) for the $z$-band filter. Each final image has a total area over which the total integration time contributes to the signal of 44 arcmin$^2$. The 3 $\sigma$ detection limits in a 2″ diameter circular aperture are $R_{\rm AB} = 27.8$, $I_{\rm AB} = 26.7$, and $z_{\rm AB} = 26.0$. The detection limits are consistent with those expected from the count rates and sky backgrounds (i.e., the uncertainties in the photometry do not have significant contributions from errors in the flat fielding or any other calibration used in the data reduction).

### 2.2. *Object Selection for the Multiobject Spectroscopy*

After the images were completely reduced and the flux calibration determined, we then made an object catalog using the galaxy photometry package SExtractor version 2.2.2 (Bertin & Arnouts 1996). Our final source catalog was constructed using the $I$-band image as the detection image with which to center the apertures and estimate the magnitudes in both the $R$ and $z$ bands. This method was used, as our goal was to find objects with large spectral breaks between the $R$ and $I$ bands, indicating that they may be at high redshifts. However, we were concerned that selecting candidate high-redshift galaxies based solely on their detection in one band might lead to spurious sources. Therefore, as a check of the centering of the apertures, the influence of the noise properties of individual colors or images, etc., we also generated catalogs using the $R$ band, $z$ band, and a simple sum of the three images as the detection images. Given the color criteria we used to select our target galaxies for follow-up spectroscopy, we noted no significant dependence on the image used to select objects other than those given by differences in the detection limits (like limiting color and source densities). The final magnitudes adopted for each of the sources are from a 2″ diameter circular aperture based on the aperture position given using the $I$-band image for source detection. Although the total imaged area was approximately 44 arcmin$^2$ we excluded sources near the edge of the frames to minimize possible flat-fielding errors, differences in sensitivity due to nonuniform exposure, or sources partially falling off the imaged region, all of which can affect the photometry. Moreover, part of the area was vignetted by the guide probe for some of the image, and this region was also excluded. Taking these into account, our sample was selected from the central $\approx$41.3 arcmin$^2$ of the final image.

As stated in § 1, our goal is to use the opacity of the IGM shortward of Ly$\alpha$ to select objects with large magnitude breaks between the $R$ and $I$ bands. Using the analysis of Madau et al. (1999), Songaila & Cowie (2002), and Fan et al. (2002) of the amount of IGM absorption expected shortward of Ly$\alpha$, along with spectrophotometric models of early star formation in galaxies (Fioc & Rocca-Volmerange 1997) and existing high-redshift quasar spectra, we determined that a color selection of $R_{\rm AB} - I_{\rm AB} \geq 1.5$ will include all sources at $z > 4.8$ (Fig. 1). This selection is mainly driven by the IGM opacity, and thus

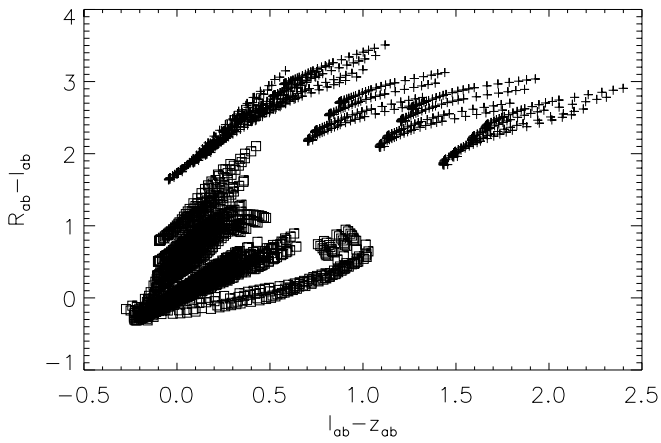


FIG. 1.—Expected locus of colors, $R_{\rm AB} - I_{\rm AB}$ vs. $I_{\rm AB} - z_{\rm AB}$, for $0.1 < z < 5.9$. The models were generated using the code from Fioc & Rocca-Volmerange (1997), were all single-burst models with ages that range from 5 Myr to 14 Gyr, and have had extinctions at $V$, $A_V = 0.1$, 0.3, 0.7, and 1.0, applied assuming the Calzetti et al. (2000) extinction law. In addition, we have applied the absorption of the IGM shortward of rest-frame Ly$\alpha$ using the prescription given in Madau et al. (1996) but modified for $z > 4.8$ to account for the additional IGM opacity above the Madau et al. (1996) estimate observed in the SDSS QSOs (Fan et al. 2002). For each redshift, all models with ages younger than the age of the universe at that redshift are shown. Galaxies with redshifts in the range $4.8 < z < 5.9$ are shown as blue squares. As can be seen, galaxies with $4.8 < z < 5.9$ span a wide range of $I_{\rm AB} - z_{\rm AB}$, but almost all are redder than $R_{\rm AB} - I_{\rm AB} \geq 1.5$, our adopted color selection. [*See the electronic edition of the Journal for a color version of this figure.*]

using an accurate estimate of it is crucial to selecting galaxies at high redshifts. Our imaging data were reliable and relatively complete to $I_{AB} = 26.25$, so our primary target selection was $I_{AB} < 26.25$ and $R_{AB} - I_{AB} \geq 1.5$. These objects could in principle be at any redshift above $z > 4.8$ but in practice are likely to be at $z < 5.8$ due to the increasing effect of IGM opacity on the observed $I$ band at increasing redshift. The IGM introduces little or no appreciable "reddening" in $I - z$ at $z = 4.8$, increasing to $\sim$1.5 mag of reddening by $z > 5.8$ in these models (Fig. 1). As $R-I$ rapidly increases with redshift above $z = 4.8$, for example, at $z = 5$, $R-I > 2$, the chosen color cut is generously blue for objects in this redshift range. Consequently, even if we have excluded some objects at $z < 5$ through our color selection, the volume that is probed by these observations will barely be affected (Fig. 2).

Given the number of slitlets that can be used in the FORS2 Mask Exchange Unit (see § 2.3), we were able to observe more than just our primary sample. Consequently, we relaxed our criteria to $I_{AB} < 26.4$ and $R-I > 1.0$, including as many objects as feasible, concentrating on those with the reddest $R-I$ colors. We expected few, if any, of the sources in this expanded sample to be at $z > 4.8$, essentially only those that had $R-I > 1.5$ but with $I_{AB} > 26.25$. Where there was space on the masks, we included extremely red objects (EROs) selected from the VLT imaging and a separate $K$-band Anglo-Australian Observatory Infrared Imager and Spectrograph 2 image (to be reported on elsewhere). One object was included as it was very much brighter in the $R$ band than in $I$ and undetected in $z$. When selecting objects on the basis of color, we did not rely solely on the SExtractor cataloged $R$-band magnitudes; we examined the $R$-band images of all objects with $I_{AB} < 26.4$ and $R_{AB} > 27.2$ by eye. This allowed us to include objects in which the $R$-band magnitudes were overestimated by SExtractor because of crowding with other objects or from unreliable background estimation. We also examined sources detected by SExtractor in the $I$ band alone, rejecting those in which the source appeared bogus. This affected only a few of the faintest objects.

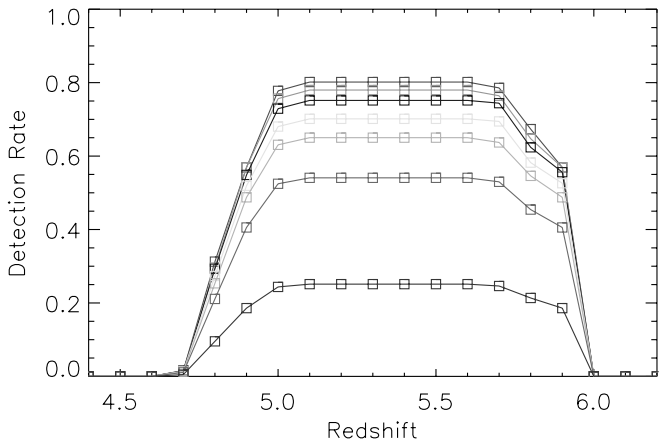


FIG. 2.—Detection rate of the galaxies as a function of magnitude and redshift. The magnitudes from top to bottom are for $I_{AB} = 23.25$, 23.75, 24.25, 24.75, 25.25, 25.75, and 26.25. The detection rate for any magnitude is reasonably uniform in the range $4.8 < z < 5.8$. Due to the small number of sources with spectroscopic redshifts, we do not plot a histogram of the redshift distribution but note that the spectroscopic redshifts are consistent with the estimated detection rate as a function of redshift. However, due to the strong night-sky emission over the wavelength range of observed Ly$\alpha$, the redshifts measured correspond mainly to regions relatively devoid of strong night-sky lines. Thus the redshift distribution is most strongly influenced by the wavelengths of the strong night sky and much less so by the selection function of the objects themselves. [*See the electronic edition of the Journal for a color version of this figure.*]

The $z$ band was used to constrain the observational priority in an attempt to remove intrinsically red objects (cool stars and substellar objects), but again, there were sufficient slitlet numbers so that this criterion was not strictly observed, and such objects were included in spectroscopy to confirm their photometric classification. In the rest of this paper, we will discuss only the objects that strictly meet the primary photometric criteria.

### 2.3. *Multiobject Spectroscopy*

Spectra of these sources were obtained using the Mask Exchange Unit (MXU) in FORS2 on UT4. Key to the success of these observations was the use of new red-enhanced MIT CCD chips, which benefitted from high quantum efficiency at red wavelengths (70% at 9000 Å) and extremely low fringe amplitudes. The observations were carried out in service mode on the nights of 2002 August 6 and 8. We observed with the 300 line mm$^{-1}$ grism blazed in the $I$ band and an OG 590 order-separating filter. The final spectra span the range of about 6000 Å to 1.1 $\mu$m for slits placed near the center of the field. The setup included two masks, each of which was observed partially on those two nights. The total integration time per mask was 4 1/3 hr. Generally, each slitlet was 10″ in total length and 1″ in width. The data were reduced by bias-subtracting frames with zero exposure time and no illumination, flat-fielded using normalized spectra of a continuum source, and wavelength-calibrated using observations through each mask of a comparison lamp. Each mask had 20 sets of exposures that were dithered along the slit. After bias subtraction and flat-fielding, the sky was subtracted using a average combination of three frames taken closest in time and then had a first-order polynomial subtracted from each column after the first pass at sky subtraction. The separate spectra for each slit were then aligned and averaged together. The spectra were then rectified to wavelength calibrate them and then flux-calibrated using the standard spectrophotometric standard LTT 7987. The excellent cosmetic quality of the chips in FORS2 along with their very high quantum efficiency and lack of fringing in the red meant that we could often spectroscopically detect very faint objects ($z_{AB} \geq 25$) to 1 $\mu$m (Fig. 3).

## 3. RESULTS

### 3.1. *Results from the Spectroscopy*

There were 18 objects that met our strict primary selection criteria of $I_{AB} < 26.25$, $R_{AB} - I_{AB} \geq 1.5$. These split neatly into two groups based on $I$-band magnitude. The first group of five had $I_{AB} < 24.5$. Three were point sources with the colors of main-sequence stars, and one had the colors and morphology of a $z \sim 1$ elliptical, with its $R_{AB} - I_{AB}$ color just making the color cut. The fifth object was stellar in appearance but had $R_{AB} - I_{AB} > 3$ and $I_{AB} - z_{AB} \sim 0.6$, making it a candidate quasar. All except one of the stellar objects, including the quasar candidate, were spectroscopically observed. None were found to be at $z > 4.8$. The candidate elliptical was also confirmed spectroscopically.

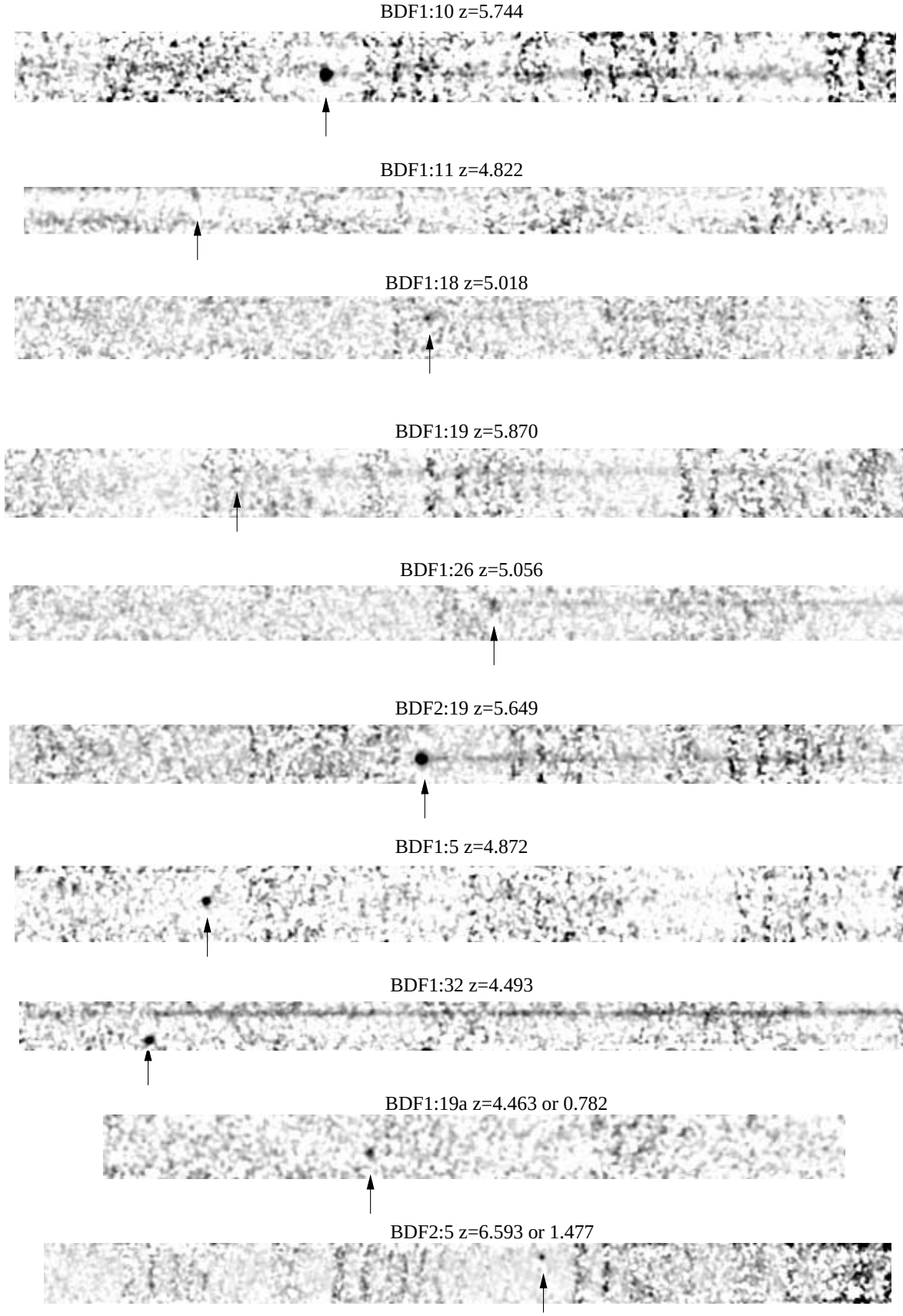


FIG. 3.—Two-dimensional spectra of the galaxies for which we have estimated the redshifts. *Top to bottom*: BDF 1:10 ($z = 5.744$); BDF 1:11 ($z = 4.822$); BDF 1:18 ($z = 5.018$); BDF 1:19 ($z = 5.870$); BDF 1:26 ($z = 5.056$); BDF 2:19 ($z = 5.649$); BDF 1:5 ($z = 4.872$); BDF 1:32 (both BDF 1:32a and 1:32b have $z \approx 4.49$); BDF 1:19a ($z = 4.46$; the blue end of the slitlet spectrum of BDF 1:19 shown near the top of the figure); and BDF 2:5 ($z = 6.59$). The bottom four galaxies are not part of the primary sample of LBGs. Each of the displayed spectra is approximately 1500 Å in length.

TABLE 1
PROPERTIES OF THE PRIMARY SAMPLE

| Designation (1) | $R_{AB}$ (2) | $I_{AB}$ (3) | $z_{AB}$ (4) | $\lambda_{line}$ (5) | $\log f_{line}$ (6) | Redshift (7) | $\log L_{line}$ (8) | $M_{AB}(1700\ \text{Å})$ (9) |
|---|---|---|---|---|---|---|---|---|
| BDF 1:9 ..... | >27.8 | 26.2 | 25.8 | | | | | −20.3 |
| BDF 1:10 ..... | >27.8 | 26.0 | 25.3 | 8191.8 | −16.61 | 5.7441 | 42.94 | −21.3 |
| BDF 1:11 ..... | >27.8 | 25.8 | 25.5 | 7078.2 | −17.80 | 4.8223 | 41.58 | −20.8 |
| BDF 1:14 ..... | >27.8 | 26.0 | 24.9 | | | | | −21.7 |
| BDF 1:18 ..... | >27.8 | 26.0 | 25.4 | 7315.5 | −17.62 | 5.0175 | 41.80 | −21.0 |
| BDF 1:19 ..... | >27.8 | 26.0 | 25.4 | 8351.4 | −17.51 | 5.8696 | 42.07 | −21.1 |
| BDF 1:26 ..... | >27.8 | 25.6 | 25.9 | 7362.0 | −17.46 | 5.0558 | 41.97 | −20.7 |
| BDF 2:12 ..... | >27.8 | 26.2 | >26.0 | | | | | > −20.5 |
| BDF 2:13 ..... | >27.8 | 26.0 | >26.0 | | | | | > −20.5 |
| BDF 2:15 ..... | >27.8 | 25.9 | >26.0 | | | | | > −20.5 |
| BDF 2:17 ..... | >27.8 | 26.2 | >26.0 | | | | | > −20.5 |
| BDF 2:19 ..... | >27.8 | 26.1 | 25.2 | 8083.0 | −16.60 | 5.6488 | 42.94 | −21.4 |
| I1020..... | >27.8 | 26.1 | >26.0 | | | | | > −20.5 |

NOTE.—Col. (1): Source name. Cols. (2)–(4): Magnitudes in the AB system. Col. (5): Wavelength of identified line in angstrom units. Col. (6): Logarithm of the integrated flux of the line in ergs $s^{-1}$ $cm^{-2}$. Col. (7): Redshift assuming the observed line is Ly$\alpha$. Col. (8): Logarithm of the total line luminosity assuming $H_0 = 70$ km $s^{-1}$ $Mpc^{-1}$, $\Omega_{matter} = 0.3$, and $\Lambda = 0.7$. Col. (9): Absolute AB magnitude at 1700 Å, calculated from the $z$-band magnitude assuming no color term. The sources without measured redshifts are assumed to be at $z = 5.3$, which is approximately at the peak selection efficiency (see Fig. 2).

The second group of 13 sources all had $25.5 < I_{AB} < 26.25$ and $R_{AB} > 27.8$. All were undetected in $R$ and half were undetected in $z$. All 13 sources are listed in Table 1 along with their redshifts when measured. We obtained spectra for 12 of these sources; the other source was excluded because of slit contention (by which we mean that the objects were aligned such that it was impossible to place two slits that would not overlap spatially and would still be long enough to provide for accurate sky subtraction). Of these sources, six have spectroscopically determined redshifts, and their spectra are shown in Figures 3 and 4. Our sample selection was optimized to detect objects with redshifts between $z = 4.8$ and 5.8. To determine this selection, we carried out an analysis similar to that presented in Steidel et al. (1999). In addition to knowing the expected colors of high-redshift galaxies, the completeness of the observations need to be determined. We made the incompleteness estimate in two ways. First, we distributed galaxies of different magnitudes and colors (effectively redshifts) randomly across the frame, then attempted to recover them with the same procedure and color selection used when making the original galaxy catalogs. This analysis was similar to that performed in Steidel et al. (1999); the only difference was that we used the actual galaxies detected with known redshifts and colors instead of model galaxies. Second, to estimate the relative influence of the possible sources of incompleteness (i.e., source confusion, incompleteness as a function of magnitude, and the influence of our color selection criteria on the completeness as a function of redshift) we determined the incompleteness in a three-step process. We determined the effective area of our images by recovering objects placed at random across the $I$-band frame. A range of magnitudes was used in order to determine the fraction of galaxies recovered. We then determined the incompleteness directly by determining the deviation of the faint galaxy surface density from a power-law fit to the source surface density as a function of magnitude over the range of magnitudes in which the data were complete (in the $I$ band, this was $22.5 < I < 25.5$). We also estimated the incompleteness as a function of redshift due to our color selection criteria. For this, we carried out a Monte Carlo simulation using the range of model parameters used in Figure 1, distributing these randomly over the redshift range 2–6.5. The results of the Steidel-like and the three-step process estimates agree within statistical uncertainties. The final results of the second method are shown in Figure 2. Given the range of confirmed redshifts, we have succeeded as expected.

Spectra of several of the other six sources showed evidence for a Lyman break in that redshift range, but none as sharp as the line emitters due to limited signal-to-noise ratios. Consequently, we do not assign these an exact redshift. Others were too faint to reliably detect spectral features in the continuum. None showed features that indicated redshifts of $z < 4.8$. Also, the redshift distribution of the line emitters is not uniform between $z = 4.8$ and 5.8 but in fact fall mainly near the low and high ends of the redshift range. This is most likely due to the wavelength distribution of the strong night-sky lines, since the redshifts measured tend to be in regions devoid of strong sky lines. Therefore, it is possible that some of the sources without spectroscopically determined redshifts are such because their redshifted Ly$\alpha$ line falls in a region of strong night-sky line emission. In what follows we refer to these 13 objects as the primary sample. The inclusion of the last object is justified in that it was only excluded from the spectroscopic sample because of a conflict in slit position with another candidate high-redshift source.

The strong line emitters in this sample of 13 are characterized by extremely high rest-frame equivalent widths, more than 30–50 Å in the rest frame. The Ly$\alpha$ line luminosities implied by line fluxes are about $4 \times 10^{41}$ to almost $10^{43}$ ergs $s^{-1}$. Using the models of Leitherer et al. (1999) and Charlot & Fall (1993) and assuming case B recombination to convert Ly$\alpha$ to H$\beta$ line luminosity, we find that UV continuum and line emission is indicative of an extremely young galaxy (ages $<10^7$–$10^8$ yr given the uncertainty in the equivalent width) and star formation rates of up to about 20 $M_\odot$ $yr^{-1}$

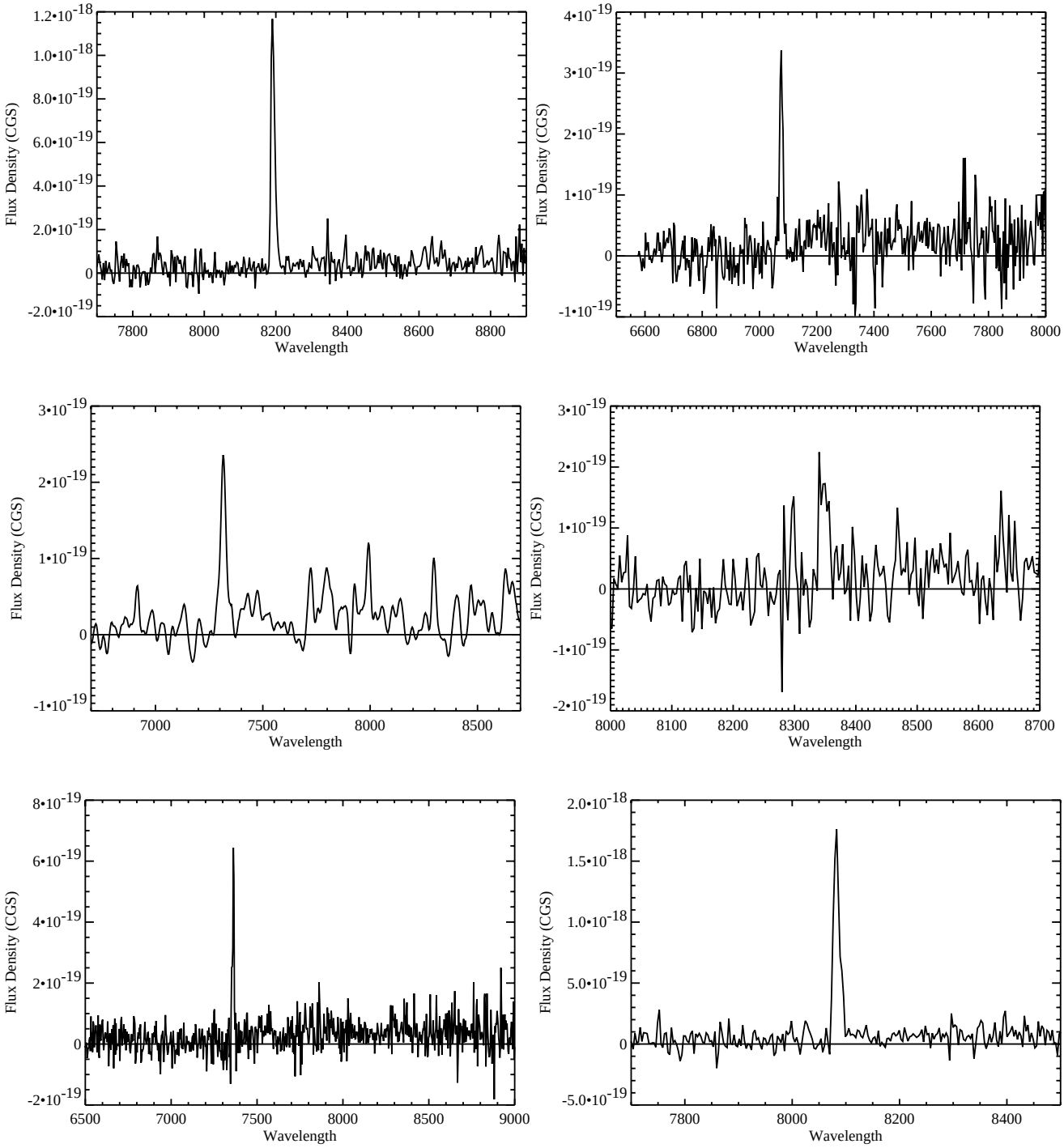


FIG. 4.—One-dimensional spectra of the spectroscopically confirmed LBGs selected to have $R_{AB} - I_{AB} > 1.5$, $I_{AB} < 26.1$, and $R_{AB} > 27.6$. *Top*: BDF 1:10 and BDF 1:11. *Middle*: BDF 1:18 and BDF 1:19. *Bottom*: BDF 1:26 and BDF 2:19. The large continuum break between $R$ and $I$ in all of the sources and the obvious line asymmetry in the strongest line emitters imply that the detected lines are likely Ly$\alpha$ emission at high redshifts.

(neither of these estimates take into account possible extinction).

None of the objects in the primary sample have spectroscopically determined redshifts below $z < 4.8$. Only one object in the expanded sample was found to be at $z > 4.8$. This had an $I$-band magnitude of $I_{AB} = 26.3$, just too faint to be included in the primary sample, and was undetected in $R$, so it had $R_{AB} - I_{AB} \geq 1.5$. It has a redshift of $z = 4.88$. This indicates that selecting objects with $I_{AB} > 25$ and $R_{AB} - I_{AB} \geq 1.5$ is a reliable and efficient way of selecting galaxies at $z > 4.8$ and out to at least $z = 5.8$, given the results of our spectroscopy.

One other object in the expanded sample, BDF 1:32b, was found to be at $z > 4$ (Table 2). This was detected in both $R$ and $I$ and had a relatively blue $R-I$ color. However, we note that BDF 1:32 lies near a bright star, which affected the photometry significantly. Practically all of the $R$-band light came from a strong emission line at 6675 Å (Fig. 3). This is taken to be Ly$\alpha$ at $z = 4.46$. Another continuum-only object in the slit 5″ north of the line emitter has a sharp

TABLE 2
OTHER GALAXIES AT $z > 4$ IN THE EXPANDED OR SERENDIPITOUS SAMPLES

| Designation (1) | $R_{AB}$ (2) | $I_{AB}$ (3) | $z_{AB}$ (4) | $\lambda_{line}$ (5) | $\log f_{line}$ (6) | Redshift (7) | $\log L_{line}$ (8) |
|---|---|---|---|---|---|---|---|
| BDF 1:5 ..... | 27.7 | 26.3 | 25.8 | 7142.5 | −17.17 | 4.8752 | 42.22 |
| BDF 2:5 ..... | >27.8 | >26.7 | >26.0 | 9229.8 | −17.32 | 6.5926 | 42.38 |
| BDF 1:19a ..... | >27.8 | >26.7 | >26.0 | 6640.9 | −16.97 | 4.4626 | 42.33 |
| BDF 1:32a ..... | 25.2 | 24.4 | 24.3 | | | 4.49 | |
| BDF 1:32b ..... | ∼25.5 | >25.7 | >26.0 | 6677.5 | −17.89 | 4.4927 | 41.42 |

NOTE.—Col. (1): Source name. Cols. (2)–(4): Magnitudes in the AB system. For BDF 1:32b both the cataloged $R$ and $I$ magnitudes were affected by poor background estimation due to the presence of a bright nearby star, hence the limit for the $I$-band magnitude. Col. (5): Wavelength of identified line in Å. Col. (6): Logarithm of the integrated flux of the line in ergs $s^{-1}$ $cm^{-2}$. Col. (7): Redshift assuming the observed line is Ly$\alpha$. For BDF 1:32a, the redshift estimate is based on the continuum break assuming it is due to Ly$\alpha$ absorption from the IGM. Col. (8): Logarithm of the total line luminosity assuming $H_0 = 70$ km $s^{-1}$ $Mpc^{-1}$, $\Omega_{matter} = 0.3$, and $\Omega_\Lambda = 0.7$.

break in the continuum at the same wavelength, with little or no continuum flux shortward of ≈6675 Å (BDF 1:32a). These two objects are therefore likely to be at the same redshift: one is a strong line emitter; the other is a continuum-only Lyman break galaxy (Fig. 3).

### 3.2. *Surface Densities of High-Redshift LBGs*

How do the luminosities and surface densities of our sources compare with those of the Lyman break galaxies in Steidel et al. (1999) at $z = 3$ and 4? Given the small area of our survey and the small number of sources, we do not attempt to determine a luminosity function for the sources. Determining the luminosity function is complicated by the diminution of the $I$-band flux from an object as the redshift increases from $z = 4.8$ to 5.8 because of the opacity of the IGM. Instead, we constructed a simulation of the expected number counts in $I_{AB}$ over this redshift range assuming no evolution in the luminosity function taken from Steidel et al. (1999) for $z \approx 3.0$ and 4.1 LBGs (converted to the cosmology $H_0 = 70$ km $s^{-1}$ $Mpc^{-1}$, $\Omega_{matter} = 0.3$, $\Omega_\Lambda = 0.7$) and that the galaxies are distributed uniformly in the *completeness-corrected* volume (i.e., the completeness correction has been applied as a function of magnitude and redshift; see Fig. 2). We assume that the absolute magnitude at 1700 Å relates directly to the observed $z$-band magnitude with no color term. We modeled the $I-z$ colors of young galaxies (from the models of Fioc & Rocca-Volmerange) over this redshift range including the effects of IGM opacity (from Madau et al. 1999; modified using the determinations from Fan et al. 2002). An approximate fit to the color of these objects is given by $I_{AB} - z_{AB} = 1.5 \times (z - 4.8)$ over the redshift range $4.8 < z < 5.8$. With these assumptions we distributed the galaxies assuming their magnitudes followed the luminosity function from Steidel et al. (1999), assigned a redshift with the appropriate difference in the distance modulus between $z = 4.1$ and the assigned redshift, and then applied the diminution due to the IGM. The incompleteness correction was included using the estimates outlined in § 3.1.

The simulated number counts, including the incompleteness as a function of magnitude and redshift, are shown in Figure 5. Above $I_{AB} < 25.5$ we have no candidate galaxies at $z > 4.8$, whereas of order 10 are predicted. Down to $I_{AB} < 26.25$, about 40 sources are predicted compared with 13 detected in our primary sample. Although the number of detected sources are below those expected if the luminosity function of UV-bright Lyman break galaxies does not evolve from $z = 3$ to $z > 5$, the differences are not highly significant except at the brightest end. Even then the cosmic variance might account for much of this difference given the relatively small area of our field. But taken at face value, our results suggest that the luminosity function at these high results has shifted to fainter magnitudes and is steeper at the bright end compared with the luminosity function at $z = 4.1$.

The estimate of any significant underdensity of sources relies predominately on the relationship between $I-z$ and

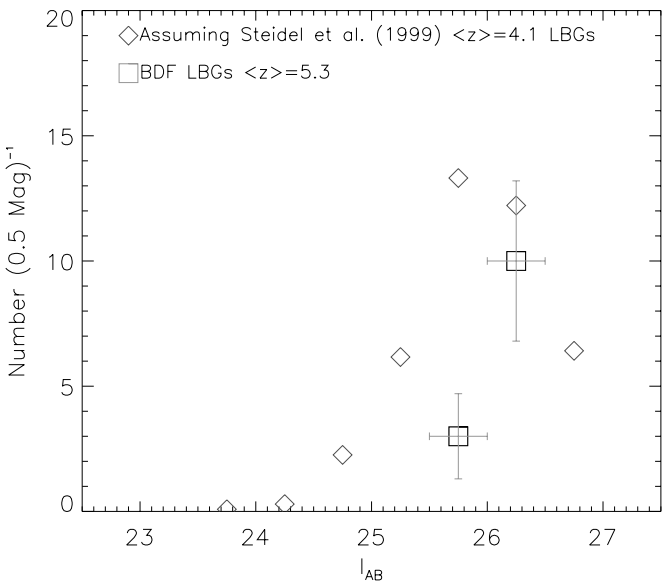


FIG. 5.—Comparison of the predicted number of LBGs at $z \approx 5.3$ and the observed number in our field. To construct this plot, we made a simple Monte Carlo simulation of the expected number of LBGs assuming that the comoving volume density of LBGs at $z \approx 3.0$ and 4.1 LBGs from Steidel et al. (1999) remained unchanged to $z \approx 5.3$, used a simple scaling for the effect of the absorption due to the IGM shortward of Ly$\alpha$ on the $I-z$ color, that the $z$-band magnitude is related to the magnitude of the LBGs at $z \approx 4.1$ through the difference in the distance modulus, and that the redshift distribution of the sources was similar to that modeled in Fig. 2 between 4.8 and 5.8. In addition, we applied the incompleteness of our data to the simulated distribution. The results of the simulation are shown as red diamonds. The green squares represent our observed number of sources in the field. The uncertainties of the observed number of galaxies are Poissonian. [*See the electronic edition of the Journal for a color version of this figure.*]

redshift. The range of $I_{AB} - z_{AB}$ colors seen in the models in Figure 1 results from the strong absorption due to the IGM with a smaller contribution from range of extinction and ages. The span in color due to redshift and IGM absorption is about 2 mag, while that due to reddening and age is about 0.5 mag for any one redshift. The range of $I_{AB} - z_{AB}$ colors observed in the galaxies of our primary sample is less than 0.2–1.1. Although the number of spectroscopically determined redshifts is small, the galaxies at $z = 5.6$–5.8 do have the reddest $I-z$ colors of our sample ($I_{AB} - z_{AB} = 0.6$ or 0.7), consistent with the dominant influence of the attentuation due to the IGM. These colors are consistent with little reddening and young ages ($\lesssim 10^8$ yr) mainly due to the strong attenuation of the IGM at the highest redshift. And since dust destroys Ly$\alpha$ preferentially and only galaxies with young ages have strong Ly$\alpha$ emission (e.g., Leitherer et al. 1999; Charlot & Fall 1993), such a conclusion is also supported by the high rest-frame equivalent widths observed in Ly$\alpha$. Given the dominant influence of the IGM opacity on the colors of the galaxies and the lack of extremely red $I-z$ colors one might be concerned about how the choice of $I_{AB} - z_{AB} = 1.5 \times (z - 4.8)$ used in our simulation might bias our conclusions. To gauge the influence of the relationship between color and redshift on the predicted numbers of LBGs, we ran the surface density simulation with a variety of coefficients for linearly relating redshift and $I_{AB} - z_{AB}$ [e.g., $I_{AB} - z_{AB} = 1.0 \times (z - 4.8)$ and $I_{AB} - z_{AB} = -0.5 + 1.0 \times (z - 4.8)$] that would be consistent with both the model and observed galaxy colors as a function of redshift. The results imply that our assumption of $I_{AB} - z_{AB} = 1.5 \times (z - 4.8)$ is conservative. For example, adopting $I_{AB} - z_{AB} = 1.0 \times (z - 4.8)$ [which is more in line with the observed range of colors and redshifts than is $I_{AB} - z_{AB} = 1.5 \times (z - 4.8)$], about 50 sources are predicted compared with the 13 detected in our primary sample, and the discrepancy at the faint magnitudes becomes significant (Fig. 6). Therefore, any relationship between color and redshift with a weaker dependence on redshift or that reaches less extreme $I_{AB} - z_{AB}$ colors at $z = 5.8$ than we have assumed, tends to increase the significance of the observed underdensity of sources compared with LBGs at lower redshifts.

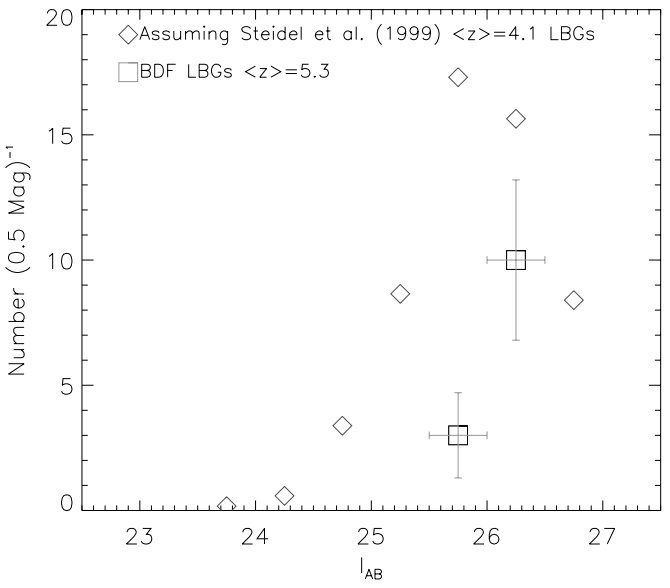


FIG. 6.—Same simulation as presented in Fig. 5, except we now have assumed that $I_{AB} - z_{AB} = 1.0 \times (z - 4.8)$. [*See the electronic edition of the Journal for a color version of this figure.*]

The justification for the analysis just presented is that the IGM has a substantial impact on the resulting magnitudes and number densities of the sources at these redshifts. Therefore, it is imperative that its effect be properly accounted for. In spite of this caveat, to further our comparison with LBGs at low redshifts, we estimated the total comoving densities and UV luminosity density from sources with $4.8 < z < 5.8$. Applying the incompleteness corrections, we find the total comoving density of sources with $M_{AB}(1700\ \text{Å}) \gtrsim -20$ of about $10^{-3.3}$ Mpc$^{-3}$. The estimated UV luminosity density is about log $\rho_{UV} \approx 25.7$ ergs s$^{-1}$ Hz$^{-1}$ Mpc$^{-3}$. Both of these estimates are approximately a factor of 3 below that estimated at $z \approx 4$ (Steidel et al. 1999). Although the correction for IGM opacity is uncertain and both the total comoving space densities and UV luminosity density strongly reflect the number densities of sources at the faintest magnitudes where the relative underdensity is small, these estimates suggest an overall decline in the number and emissivity of sources from $z \approx 4$ to 5.3, consistent with our simulations.

A possible cause of the discrepancy in the expected number of sources at $z \approx 5.3$ and 4 could be the effects of surface brightness dimming, which results in systematically underestimating the magnitudes of galaxies at high redshift. To provide an estimate of the size of the effect, the relative difference in surface brightness between $z = 4.1$ and 5.3 is about 1 mag arcsec$^{-2}$. However, surface brightness dimming is unlikely to have a substantial impact for several reasons. The images used to select the galaxies for this survey are about 1 mag deeper than the ground-based images used in, for example, Steidel et al. (1999), thus compensating somewhat for the differences in surface brightness of the two galaxy samples. In addition, we note that none of the objects are resolved significantly in the 0.″7 seeing of the images. In an analysis of similarly selected galaxies from the Chandra Deep Field–South with deep *Hubble Space Telescope* (*HST*) Advanced Camera for Surveys images, galaxies have half-light radii that range from unresolved at *HST* resolution to less than a few tenths of an arcsecond (M. Bremer et al. 2003, in preparation; Stanway, Bunker, & McMahon 2003). Moreover, if all of the galaxies have a similar morphology regardless of their magnitude, one would expect the fainter sources to have their magnitudes significantly underestimated compared with the brighter sources. This is because brighter galaxies will be detected over a broader range of surface brightness than that of fainter galaxies. Our results suggest that the difference in the source densities is significant for the bright high-redshift galaxies and much less so for the faint sources. Thus, surface brightness dimming is unlikely to play a significant role in explaining the paucity of bright sources.

We also investigated the constraints that these results put on the QSO luminosity function at these high redshifts. We detected no broad-line sources (QSOs) in our spectra. Assuming that the redshift coverage is between 4.8 and 5.8, and applying the completeness correction discussed above, we find that the comoving density of QSOs must be less than about $10^{-4.8}$ Mpc$^{-3}$ for $-23.5 \lesssim M_B \lesssim -20.5$. (Due to the completeness corrections, the exact density depends on the

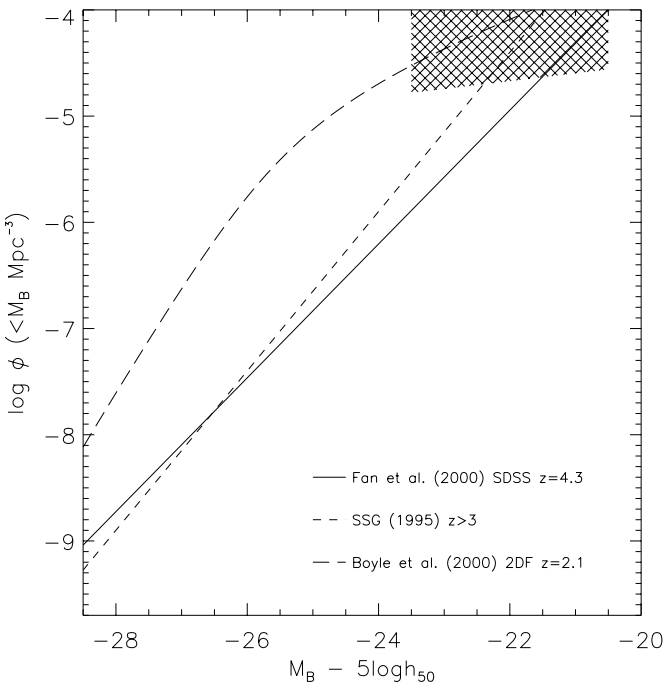


FIG. 7.—Comparison of compilations of QSO luminosity functions with the upper limits we derive given that there are apparently no QSOs in the 44 arcmin$^2$ (effectively smaller after applying the corrections of incompleteness) region of the survey field. The lines are the luminosity function from Fan et al. (2001) for luminous QSOs in the Sloan Digital Sky Survey; Schmidt et al. (1995) from the Palomar Grism Transit Survey; and Boyle et al. (2000) $z \approx 2.1$ QSOs from the 2 Degree Field survey. The hatched region approximately indicates the region where we have not detected any QSOs. For comparison purposes, we have adopted the cosmology of $H_0 = 50$ km s$^{-1}$ Mpc$^{-1}$ and $\Omega = 1$. [*See the electronic edition of the Journal for a color version of this figure.*]

magnitude; see Fig. 7.) The *B*-band magnitude was estimated assuming a power-law slope for the QSO spectrum of $-0.5$ (Schmidt, Schneider, & Gunn 1995; Fan et al. 2001). This limit on the comoving space density implies that the QSO luminosity function as observed by Schmidt et al. (1995) and Fan et al. (2001), while already flatter than the lower redshift luminosity functions, must turnover at $M_B \lesssim -23$.

Several other galaxies at these redshifts have been discovered in previous studies, but the diversity in galaxy selection methods make the studies difficult to compare with ours. Those selected by lensing (Ellis et al. 2001) or narrowband imaging (Hu et al. 2002; Rhoads et al. 2003) have continuum magnitudes that are generally below our *I*-band limits. Others were serendipitously discovered (Dey et al. 1998) or based on optical/IR colors (Weymann et al. 1998). Techniques comparable to ours were used by Dey et al. (1998) and Spinrad et al. (1998) to detect $z = 5.3$ galaxies in individual Keck and *HST* images. The pair of galaxies detected by Spinrad et al. in the Hubble Deep Field–North (HDF-N) would have been seen in our ground-based imaging as an individual source. Both this and the galaxy detected by Dey et al. (1998) would have been discovered by us had they fallen within our field. Given the relative field sizes and exposure depths, the discovery of these objects is entirely consistent with the surface density of galaxies at $z > 4.8$ in this study.

Wide-field narrowband surveys for line-emitting galaxies (e.g., Rhoads & Malhotra 2001; Ouchi et al. 2003) are efficient at detecting the most extreme line emitters at high redshift. None of the galaxies in Rhoads et al. (2003) have sufficient line flux alone to be detected by us in the broadband filters given our flux limit. For example, a flux of $5 \times 10^{-17}$ ergs$^{-1}$ s$^{-1}$ cm$^{-2}$ is below our detection limit in both *I* and *z* bands, assuming that a majority of the flux from the objects in these bands arises from a Ly$\alpha$ line. Adopting the figures in Rhoads et al. (2003), assuming a 3 $\sigma$ *I*-band continuum detection limit of $I_{AB} > 25.9$, we would expect about four objects (taking into account the incompleteness) with line fluxes of more than $1.5 \times 10^{-17}$ ergs$^{-1}$ s$^{-1}$ cm$^{-2}$ and $I_{AB} > 25.9$ in our central field of 41.3 arcmin$^2$. The Rhoads et al. (2003) survey is sensitive to the most extreme line emitters; our continuum-detected sources in the primary sample typically have lower Ly$\alpha$ equivalent widths (although we note that several of them, including the strongest of the line emitters, have equivalent widths >100 Å). Formally, we detect two line emitters with line fluxes greater than $1.5 \times 10^{-17}$ ergs$^{-1}$ s$^{-1}$ cm$^{-2}$ and $I_{AB} > 25.9$. However, both galaxies are $I_{AB} \approx 26$, barely below the 3 $\sigma$ continuum detection limit of Rhoads et al. (2003). Thus while consistent within the uncertainties, it is likely that there are more objects with fainter continuum magnitudes similar to the Rhoads et al. (2003) sources but with lower line fluxes in our field. If we assume that the Ly$\alpha$ luminosity density measures the unobscured star formation density, it is therefore likely that a significant fraction (probably most) of the star formation occurring in our field at $z > 4.8$ happens in objects fainter than our magnitude limit. If so, the UV luminosity density produced by these objects is also likely to be more than that produced by objects above our magnitude limit.

### 3.3. *Serendipitously Detected Line Emitters: The Highest Redshift Galaxy?*

Along with objects that we deliberately targeted, we also detected two potentially high-redshift line-only sources serendipitously in our slitlets. The first was a line detected at 6640.9 Å in the same slitlet as BDF 1:19 (see Fig. 3 and Table 2). The second was found in a slitlet placed to fill up empty area on the slit mask (BDF 2:5). The line is at an observed wavelength of 9229.8 Å (see Fig. 3 and Table 2), which, assuming the detected line is redshifted Ly$\alpha$, would make it the highest redshift galaxy known (see Hu et al. 2002) at $z = 6.6$. However, the lack of discernible continuum emission makes this identification uncertain. The line is too weak to have a significant asymmetry in our data. It could be a low-redshift [O II] $\lambda$3727 emitter at $z = 1.4765$. If so, the upper limit of $z_{AB} = 26.0$ implies that it would have a rest-frame $U_{AB} < -17.5$ and a rest-frame equivalent width $\gg 50$ Å. Both numbers are extreme but not completely out of the question. Tresse et al. (1999) have shown that in the local universe, while such extreme equivalent widths are generally rare ($\ll$10% of galaxies are so extreme), high equivalent widths become more common in low-luminosity galaxies. Although the identification of the line as Ly$\alpha$ is not certain, we note that the redshift is no less secure than other line-only high-redshift galaxy candidates in the literature or those with very marginal single-band continuum detections.

## 4. DISCUSSION

Recently, Ferguson et al. (2002) have used the analysis of Shapley et al. (2001) and Papovich, Dickinson, & Ferguson (2001) to estimate the possible contribution of LBGs at $z \approx 4$ to the reionization of the universe. They argue that for reasonable assumptions, e.g., the relatively young age and insufficient comoving space density, LBGs at $z \approx 4$ are unlikely to be the progeny of the sources that reionized the universe. They also show that if the luminosity function of the LBGs does not evolve between the reionization epoch and $z = 3$, then they cannot provide the bulk of the UV photons that reionize the universe. The higher the redshift of reionization, the larger the deficit.

We find that there may be a decline in the number of luminous star-forming galaxies from $z \approx 3.0$ and 4.1 (Steidel et al. 1999) to $z \approx 5.3$. The number of sources we observe at $I_{AB} < 25.5$ is less than expected (zero observed and about 10 predicted) for a constant comoving density of sources over that redshift interval. Our calculated UV photon density for our primary sample over the redshift range $4.8 < z < 5.8$ falls below that of $z \sim 3$ LBGs, insufficient to ionize the IGM in the observed volume. Another source of UV photons is required. Moreover, these sources are observed within only a few hundred million years after reionization (assuming this happens at $z < 7$–10). For galaxies such as those in our primary sample to provide the bulk of reionizing photons, a dramatic and unlikely decrease in their comoving density would have to occur over this short timescale. For this deficit to be accounted for by cosmic variance, the field would have to be considerably more than an order of magnitude underluminous relative to the average field at $z > 5$.

Consequently, our results strongly imply that bright galaxies did not provide the bulk of UV photons that reionized the universe and that their number density may have declined significantly. For reionization, the majority of the photons must come from galaxies fainter than our flux limit [with absolute magnitudes of $M_{AB}(1700\ \text{Å}) \gtrsim -21$], or from brighter active galactic nuclei (AGNs) outside the $\sim$40 arcmin$^2$ field of view. Theoretically, a population of quasars with $I_{AB} \sim 24$ (10–100 times fainter than the known $z > 5$ Sloan Digital Sky Survey quasars) and a surface density of around 100 deg$^2$ could keep the volume in the range $4.8 < z < 5.8$ ionized without appearing in our field. This would require a bizarre quasar luminosity function at $z > 5$, with a steep slope over the brighter parts (to provide a high enough density of sources to cause the ionization) and then a sharp drop, to avoid more numerous, fainter sources in fields such as ours (Fig. 7) or in the HDF. However, for any reasonable quasar luminosity function (i.e., one that is like those observed for lower redshift QSOs), one would then expect several fainter AGNs at such redshifts within our field, which we do not find. Similarly, Conti et al. (1999) found no quasars in the HDF at $z > 4$ to very faint magnitudes, making this possibility extremely unlikely.

This leads to the conclusion that the bulk of the photons that reionize the universe arise from galaxies fainter than our flux limit, those with $M_{AB}(1700\ \text{Å}) > -21$ and from galaxies with generally lower Ly$\alpha$ equivalent widths. Our interpretation of the results of Rhoads et al. (2003) supports this, assuming that the bulk of the sources in the Rhoads et al. (2003) sample are Ly$\alpha$ emitters at $z = 5.7$.

We wish to thank the staff at ESO Garching and on Paranal for obtaining these data. More crucially, we also applaud their initiative and efficiency in these data immediately available to us. Specifically, we would like to thank Martino Romaniello and Paola Sartoretti for their dedication and hard work on our behalf. We thank the referee for his/her insightful and helpful comments.

## REFERENCES

Bertin, E., & Arnouts, S. 1996, A&AS, 117, 393
Boyle, B. J., Shanks, T., Croom, S. M., Smith, R. J., Miller, L., Loaring, N., & Heymans, C. 2000, MNRAS, 317, 1014
Calzetti, D., Armus, L., Bohlin, R. C., Kinney, A. L., Koornneef, J., & Storchi-Bergmann, T. 2000, ApJ, 533, 682
Charlot, S., & Fall, S. M. 1993, ApJ, 415, 580
Ciardi, B., Stoehr, F., & White, S. D. M. 2003, MNRAS, submitted (astro-ph/0301293)
Conti, A., Kennefick, J. D., Martini, P., & Osmer, P. S. 1999, AJ, 117, 645
Dey, A., Spinrad, H., Stern, D., Graham, J. R., & Chaffee, F. H. 1998, ApJ, 498, L93
Ellis, R., Santos, M. R., Kneib, J.-P., & Kuijken, K. 2001, ApJ, 560, L119
Fan, X., et al. 2001, AJ, 122, 2833
———. 2002, AJ, 123, 1247
Ferguson, H. C., Dickinson, M., & Papovich, C. 2002, ApJ, 569, L65
Fioc, M., & Rocca-Volmerange, B. 1997, A&A, 326, 950
Hamuy, M., Suntzeff, N. B., Heathcote, S. R., Walker, A. R., Gigoux, P., & Phillips, M. M. 1994, PASP, 106, 566
Hu, E. M., Cowie, L. L., McMahon, R. G., Capak, P., Iwamuro, F., Kneib, J.-P., Maihara, T., & Motohara, K. 2002, ApJ, 568, L75
Landolt, A. U. 1992, AJ, 104, 340
Leitherer, C., et al. 1999, ApJS, 123, 3
Loeb, A., & Barkanna, R. 2001, ARA&A, 39, 19
Madau, P., Ferguson, H. C., Dickinson, M. E., Giavalisco, M., Steidel, C. C., & Fruchter, A. 1996, MNRAS, 283, 1388
Madau, P., Haardt, F. R., & Rees, M. J. 1999, ApJ, 514, 648
Ouchi, M., et al. 2003, ApJ, 582, 60
Papovich, C., Dickinson, M., & Ferguson, H. C. 2001, ApJ, 559, 620
Rhoads, J. E., Dey., A., Malhotra, S., Stern, D., Spinrad, H., Jannuzi, B. T., Dawson, S., & Brown, M. 2003, AJ, 125, 1006
Rhoads, J. E., & Malhotra, S. 2001, ApJ, 563, L5
Schlegel, D. J., Finkbeiner, D. P., & Davis, M. 1998, ApJ, 500, 525
Schmidt, M., Schneider, D. P., & Gunn, J. E. 1995, AJ, 110, 68
Shapley, A. E., Steidel, C. C., Adelberger, K. L., Dickinson, M., Giavalisco, M., & Petini, M. 2001, ApJ, 562, 95
Sokasian, A., Abel, T., Hernquist, L., & Springel, V. 2003, preprint (astro-ph/0303098)
Songaila, A., & Cowie, L. L. 2002, AJ, 123, 2183
Spinrad, H., Stern, D., Bunker, A., Dey, A., Lanzetta, K., Yahil, A., Pascarelle, S., & Fernández-Soto, A. 1998, AJ, 116, 2617
Stanway, E. R., Bunker, A. J., & McMahon, R. G. 2003, MNRAS, 342, 439
Steidel, C. C., Adelberger, K. L., Giavalisco, M., Dickinson, M., & Pettini, M. 1999, ApJ, 519, 1
Stern, D., & Spinrad, H. 1999, PASP, 111, 1475
Sullivan, M., Treyer, M. A., Ellis, R. S., Bridges, T. J., Milliard, B., & Donas, J. 2000, MNRAS, 312, 442
Tresse, L., Maddox, S., Loveday, J., & Singleton, C. 1999, MNRAS, 310, 262
Weymann, R. J., Stern, D., Bunker, A., Spinrad, H., Chaffee, F., Thompson, R. I., & Storrie-Lombardi, L. J. 1998, ApJ, 505, L95